Oligogalacturonide production upon Arabidopsis thaliana – Botrytis cinerea interaction

Aline Voxeur, Olivier Habrylo, Stephanie S. Guenin, Fabien Miart, Marie-Christine Soulié, Christophe Rihouey, Corinne Pau-Roblot, Jean-Marc J.-M. Domon, Laurent Gutierrez, Jérome Pelloux, et al.

▶ **To cite this version:**

Aline Voxeur, Olivier Habrylo, Stephanie S. Guenin, Fabien Miart, Marie-Christine Soulié, et al.. Oligogalacturonide production upon Arabidopsis thaliana – Botrytis cinerea interaction. Proceedings of the National Academy of Sciences of the United States of America, 2019, 116 (39), pp.19743-19752. ⟨10.1073/pnas.1900317116⟩. ⟨hal-02351884⟩

HAL Id: hal-02351884

https://normandie-univ.hal.science/hal-02351884v1

Submitted on 6 Nov 2019

HAL is a multi-disciplinary open access archive for the deposit and dissemination of scientific research documents, whether they are published or not. The documents may come from teaching and research institutions in France or abroad, or from public or private research centers.

L'archive ouverte pluridisciplinaire **HAL**, est destinée au dépôt et à la diffusion de documents scientifiques de niveau recherche, publiés ou non, émanant des établissements d'enseignement et de recherche français ou étrangers, des laboratoires publics ou privés.

HAL Authorization

Oligogalacturonide production upon *Arabidopsis thaliana–Botrytis cinerea* interaction

Aline Voxeur[a], Olivier Habrylo[b], Stéphanie Guénin[c], Fabien Miart[a], Marie-Christine Soulié[a,d], Christophe Rihouey[e], Corinne Pau-Roblot[b], Jean-Marc Domon[b], Laurent Gutierrez[c], Jérôme Pelloux[b], Grégory Mouille[a], Mathilde Fagard[a], Herman Höfte[a], and Samantha Vernhettes[a,1]

[a]Institut Jean-Pierre Bourgin, Institut National de la Recherche Agronomique, AgroParisTech, CNRS, Université Paris-Saclay, 78000 Versailles, France; [b]EA3900-BIOPI Biologie des Plantes et Innovation, FR CNRS 3417, Université de Picardie Jules Verne, 80039 Amiens, France; [c]Centre de Ressources Régionales en Biologie Moléculaire, Université de Picardie Jules Verne, 80039 Amiens, France; [d]Sorbonne Universités, Pierre et Marie Curie Université Paris 06, UFR 927, 75005 Paris, France; and [e]Polymères Biopolymères Surfaces, Normandie Université, UNIROUEN, Institut National des Sciences Appliquées Rouen, CNRS, UMR 6270, 76000 Rouen, France

Edited by Kenneth Keegstra, Michigan State University, East Lansing, MI, and approved August 16, 2019 (received for review January 8, 2019)

Despite an ever-increasing interest for the use of pectin-derived oligogalacturonides (OGs) as biological control agents in agriculture, very little information exists—mainly for technical reasons—on the nature and activity of the OGs that accumulate during pathogen infection. Here we developed a sensitive OG profiling method, which revealed unsuspected features of the OGs generated during infection of *Arabidopsis thaliana* with the fungus *Botrytis cinerea*. Indeed, in contrast to previous reports, most OGs were acetyl- and methylesterified, and 80% of them were produced by fungal pectin lyases, not by polygalacturonases. Polygalacturonase products did not accumulate as larger size OGs but were converted into oxidized GalA dimers. Finally, the comparison of the OGs and transcriptomes of leaves infected with *B. cinerea* mutants with reduced pectinolytic activity but with decreased or increased virulence, respectively, identified candidate OG elicitors. In conclusion, OG analysis provides insights into the enzymatic arms race between plant and pathogen and facilitates the identification of defense elicitors.

oligogalacturonides | plant–pathogen interaction | *Arabidopsis thaliana* | *Botrytis cinerea* | pectin lyase

The cell wall forms the first line of defense in the interaction of plants with their microbial environment. Cell walls consist of complex polysaccharide networks, which combine multiple functional properties such as strength (to resist turgor pressure), extensibility (to allow growth), as well as protection against microbial attack. Such protection involves so called "basal immunity," which is triggered upon recognition of pathogen-associated molecular patterns but also of plant-derived molecules associated with infection, referred to as damage-associated molecular patterns (DAMPs). The latter include cell wall-derived oligosaccharides with elicitor activity (also called oligosaccharins) (1) that are produced during infection with microbes and, in particular, necrotrophic bacteria and fungi, which feed on cell walls and have large arsenals of cell wall-degrading enzymes (2).

A major source of cell wall-derived DAMPs are pectins. The pectic polymer, homogalacturonan (HG) for example, represents in *Arabidopsis* 20% of the wall of growing cells. HG is a linear polymer of α-1-4–linked galacturonic acid (GalA) residues secreted in a methylesterified (on C6) and often acetylesterified (on C2 and/or C3) form (3), which can be enzymatically deacetylesterified by pectin acetylesterases and demethylesterified by pectin methylesterases (PMEs) *in muro* (4). Demethylesterification exposes the polymer to degradation by polygalacturonases (PGs) and pectate lyases (PLs, that cleave unmethylesterified HG by β-elimination, thus generating an unsaturated bond at the nonreducing end), which can be of plant or fungal origin. HG demethylesterification plays a key role in the control of cell wall rheology underlying plant growth (5). In addition, HG turnover generates oligogalacturonides (OGs), some of which act as DAMPs or, in certain conditions, may have a signaling role in development. Indeed, treatment with unmethylesterified OGs of degree of polymerization (DP) 10 to 15 elicits strong immune responses but can also promote tomato fruit ripening by triggering ethylene production (6–12). In addition, unmethylesterified GalA trimers or tetramers can promote immunity and may have a role in skotomorphogenesis (13–15). Despite considerable interest for OG signaling in plant immunity and the commercial use of OGs as natural defense stimulators, very little is known about the OGs that are actually produced during fungal infection. So far, only 1 study reported on such in vivo-produced OGs (16). This study revealed the structure of a few pectin fragments in tomato fruit infected with the necrotrophic fungus *Botrytis cinerea* that causes gray mold disease. The production of these OGs implied the activity of PGs, PMEs and, surprisingly, pectin lyases (PNLs), fungal enzymes that cleave methylesterified HG through a β-elimination mechanism. The study did not address potential elicitor activities of these OGs.

Here we developed a sensitive analytical method based on the separation of oligosaccharides combined with accurate determination of their sizes and acetylesterification and methylesterification patterns using MS/MS. This method reveals the global OG composition of plant samples. Surprisingly, the analysis of the OGs during different stages of *B. cinerea* infection of *Arabidopsis thaliana* leaves failed to detect the accumulation of the accumulation of the unmethylesterified DP10 to -15 OGs that were previously shown to have elicitor activity. Instead, despite the abundance of PGs in *B. cinerea*, 80% of the OGs were the product of fungal PNLs, 1 of which was characterized in vitro and shown to cleave highly methylesterified

Significance

Oligogalacturonides (OGs), oligomers of α-1,4–linked galacturonic acid generated during plant infection by necrotrophic fungi, have been proposed to trigger plant basal immunity when they are applied exogenously to plant tissues. However, very little information exists on the structure and activity of the OGs that really accumulate during pathogen infection. This report reveals features of OGs generated during infection of *Arabidopsis thaliana* with the fungus *Botrytis cinerea* and identifies potential candidate OG elicitors.

Author contributions: A.V., J.P., G.M., M.F., H.H., and S.V. designed research; A.V., O.H., S.G., F.M., M.-C.S., C.R., C.P.-R., J.-M.D., and S.V. performed research; A.V. contributed new reagents/analytic tools; A.V., O.H., S.G., F.M., M.-C.S., C.R., C.P.-R., J.-M.D., L.G., and S.V. analyzed data; and A.V., O.H., L.G., H.H., and S.V. wrote the paper.

The authors declare no conflict of interest.

This article is a PNAS Direct Submission.

Published under the PNAS license.

Data deposition: Affymetrix Microarray data have been deposited in the Gene Expression Omnibus (GEO) database, https://www.ncbi.nlm.nih.gov/geo/ (accession no. GSE120933).

[1]To whom correspondence may be addressed. Email: samantha.vernhettes@inra.fr.

This article contains supporting information online at www.pnas.org/lookup/suppl/doi:10.1073/pnas.1900317116/-/DCSupplemental.

HG. We also found that most nonmethylesterified PG products were oxidized *in muro*, probably by recently described plant oxidases (17). Finally, the comparison of the OGs generated by a collection of *B. cinerea* mutants affected in pectinolysis led to the identification of specific PNL-produced OGs, the accumulation pattern of which was associated with reduced virulence and a specific gene-expression pattern *in planta*. These findings illustrate the evolutionary enzymatic arms race between plant and fungus, where the 2 partners, respectively, aim for detection and hiding of pathogen-associated oligosaccharide cues.

Results

Development of a Sensitive Separative Method for OG Characterization. In a first experiment, OGs were analyzed in the hydrolysis products of commercial citrus pectins (degree of methylesterification [DM] 60) (18) digested for 20 h with *Aspergillus aculeatus* PG. OGs were separated using hydrophilic interaction liquid chromatography (HILIC) (19–21), and characterized using high-resolution mass spectrometry (HR-MS) in negative mode. Although a number of methylesterified and nonmethylesterified GalA oligomers originating from the HG backbone could be distinguished in the HILIC elution pattern (*SI Appendix*, Fig. S1*A*), non- or poorly methylesterified OGs were insufficiently separated in broad peaks, resulting in low MS sensitivity. To improve the separation power, we developed a high-performance size-exclusion chromatography (HP-SEC)-MS–based method, which yielded sharper peaks (a few seconds), resulting in a higher signal-to-noise ratio relative to the HILIC separation (Fig. 1*A* and *SI Appendix*, Fig. S1*B*). This method allowed the DP and methylesterification pattern of each OG to be determined (up to DP16) (*SI Appendix*, Fig. S1*C*) based upon accurate mass annotation, isotopic pattern, and MS/MS analysis (*SI Appendix*, Fig. S2 and Table S1).

It was surprising to see that the retention time was not only determined by the DP but also by the methylesterification status of the OG (Fig. 1*A* and *SI Appendix*, Table S1), methylesterified OGs eluting later (corresponding to a smaller hydrodynamic volume) than their unmethylesterified counterparts. In contrast, the presence of the bulkier acetylester groups did not affect the retention time as shown by the analysis of OGs produced from highly acetylesterified sugar beet pectins (Fig. 1*B* and *SI Appendix*, Table S1). This indicates that methylesterification, unlike acetylesterification, can reduce the hydrodynamic volume of the OGs. The structural basis for this effect was revealed by the analysis of OGs that did not follow this rule (Fig. 1*C* and *SI Appendix*, Fig. S3 and Table S1), such as $GalA_3Me_2$, which coeluted with, not after, $GalA_3Me$ (GalA-GalAMe-GalA) and $GalA_4Me_3$, which coeluted with $GalA_4Me_2$ (GalA-GalAMe-GalAMe-GalA). Comparison of the structures (Fig. 1*C*) showed that OGs with 2 adjacent unmethylesterified GalAs systematically eluted earlier than OGs of the same size lacking this feature. The increased hydrodynamic volume can therefore be attributed to the electrostatic repulsion between 2 adjacent carboxylic functions, making the OG more extended (Fig. 1*C*).

OG Analysis to Characterize Pectinolytic Activities of *B. cinerea*. The *B. cinerea* genome encodes a large array of putative pectinolytic enzymes: 13 PGs, 5 PMEs, 2 PLs, and 5 PNLs. Knockout mutants

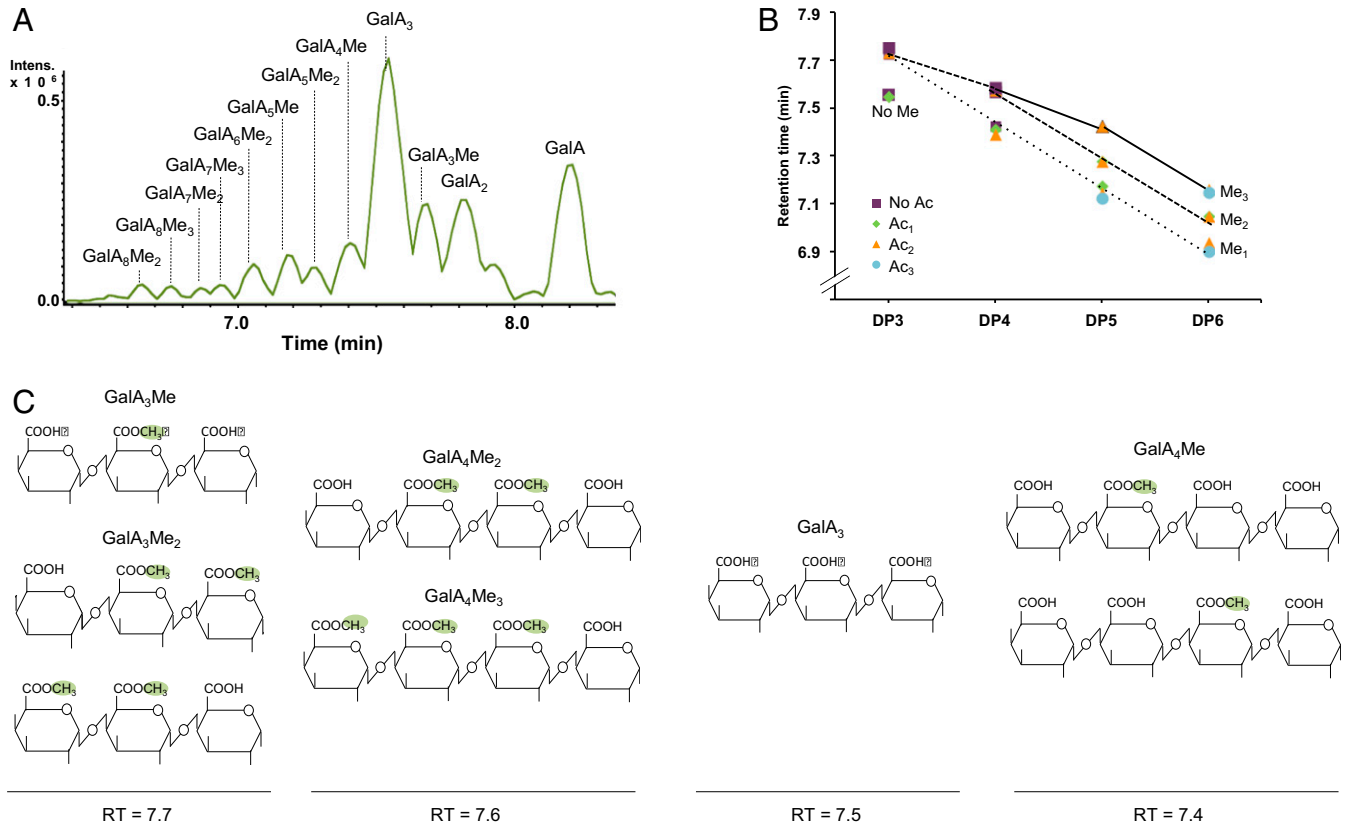

Fig. 1. A sensitive and HP-SEC method for separating complex mixes of OGs. (*A*) Base peak chromatogram obtained by LC-MS analysis in negative ionization mode of various methylesterified OGs obtained following digestion of citrus pectins by commercial PG from *A. aculeatus*. (*B*) Impact of the presence of methyl- and acetylesters on the retention time (RT) of OGs. OGs were obtained from sugar beet pectins digested by the commercial *A. aculeatus* PG. (*C*) Comparison of the structures of methylesterified OGs with a DP from 3 to 4 released by *A. aculeatus* PG and their respective RT in minutes. Positions of methyl groups are indicated according to the HG structure (3). OGs are named $GalA_xMe_yAc_z$. Subscript numbers indicate the DP and the number of methyl- and acetylester groups, respectively. Ac, acetylester group; Intens., signal intensity; Me, methylester group. Green color indicates the position of methylester groups.

were obtained for 6 PGs (22) (BcPG1 to -6) and 2 PMEs (BcPME1 and -2) (23). Their analysis showed that BcPG1 and -2 are necessary for full virulence on various plant species (24, 25), while BcPME1 and -2 are dispensable for normal virulence, at least on tomato and grapevine leaves or pear fruit (23). The activities of the 5 PGs (BcPG1 to -4, and -6) were previously characterized on polygalacturonic acid (25). Here, we used a more complex methylesterified substrate (citrus pectins, DM60) to study in more detail the activity of 2 PGs, BcPG2 and -3, representative of single-attack (nonprocessive) and multiple-attack (processive) enzymes, respectively. The former cleaves only once after formation of the enzyme–substrate complex and releases OGs of varying DPs, whereas the latter attacks the substrate multiple times and releases GalA and short OGs already from the start of the reaction (*SI Appendix*, Fig. S4).

We first purified both PGs from recombinant *Pichia pastoris* liquid cultures and incubated the enzymes with citrus pectins. After 20 h of digestion, both PGs produced mainly GalA, non-methylesterified dimers ($GalA_2$), and trimers ($GalA_3$) (Fig. 2*A*), as well as small amounts of methylesterified OGs. As expected, whereas the nonprocessive enzyme BcPG2 generated mainly $GalA_2$ and $GalA_3$, the processive BcPG3 produced primarily GalA and $GalA_2$. Such processive PG activity requires fully demethylesterified HG stretches, which are generated by (processive) plant PMEs. The presence of methylesterified OGs (up to 3 methylester groups in $GalA_5Me_3$ or $GalA_6Me_3$), however, indicates that both PGs can also cleave partially demethylesterified stretches. We next studied the combined activity of BcPME1 and BcPG2 or BcPG3. BcPME1 enhanced almost 5 times the production of GalA, $GalA_2$, and $GalA_3$ by BcPG2 and completely suppressed the accumulation of methylesterified OGs (Fig. 2*A* and *SI Appendix*, Fig. S4). In contrast, BcPME1 had a much more limited impact on the overall BcPG3 activity but promoted a shift from GalA + $GalA_2$ toward $GalA_2$ + $GalA_3$ for the most abundant OGs. Interestingly, some higher DP OGs, including $GalA_6Me_3$, resisted further digestion (Fig. 2*A* and *SI Appendix*, Fig. S4), suggesting that this OG is a poor substrate for both BcPME1 and BcPG3. Together, these results confirm that nonprocessive BcPG2 requires—and BcPG3 has a preference for—substrates of at least DP4 (25), but also show that their substrates can be partially methylesterified. In addition, they show that nonprocessive BcPME1 greatly enhances the number of cleavage sites for nonprocessive PG activities but, as expected, does not enhance the processive PG activity of BcPG3. Finally, they show that BcPME1 demethylesterifies both the HG polymer and OGs, even the trimers, except for $GalA_6Me_3$, which, for an unknown reason, is more recalcitrant to the enzyme.

We next used OG analysis to study the global *B. cinerea* pectinolytic activity. To this end, citrus pectins were incubated with *B. cinerea* spores and the OGs were analyzed over time. After 6 h of incubation, only a very small amount of OGs was detected (Fig. 2*B*). After 16 h, primarily $GalA_2$ and $GalA_3$ but also methylesterified OGs from DP4 to -7 had accumulated. Since purified BcPG2 and BcPG3 did not produce such methylesterified oligomers in large amounts, the production of these OGs most likely involved other pectinolytic enzymes. At 24 h, the relative amount of $GalA_2$ had increased and that of methylesterified OGs from DP4 to -7 had decreased. This confirms that *B. cinerea* PMEs and PGs can use OGs as a substrate.

OGs Released upon *B. cinerea*–*A. thaliana* Interaction. So far, we have shown the activity of *B. cinerea* and 3 of its purified enzymes on citrus pectins, which is a complex but inert substrate. We next investigated how the interaction with living plant cells affects the pectinolytic activity of the fungus. Previous studies have shown that plants produce defensive PG-inhibiting proteins (PGIPs) that attenuate the activity of fungal PGs (26). This is thought to promote the accumulation of large unmethylesterified OGs with elicitor activity (27), as observed for instance in *A. thaliana* upon coexpression of a PGIP with a fungal PG. However, very little is known on the OGs that are actually produced during the interaction of *B. cinerea* with its host.

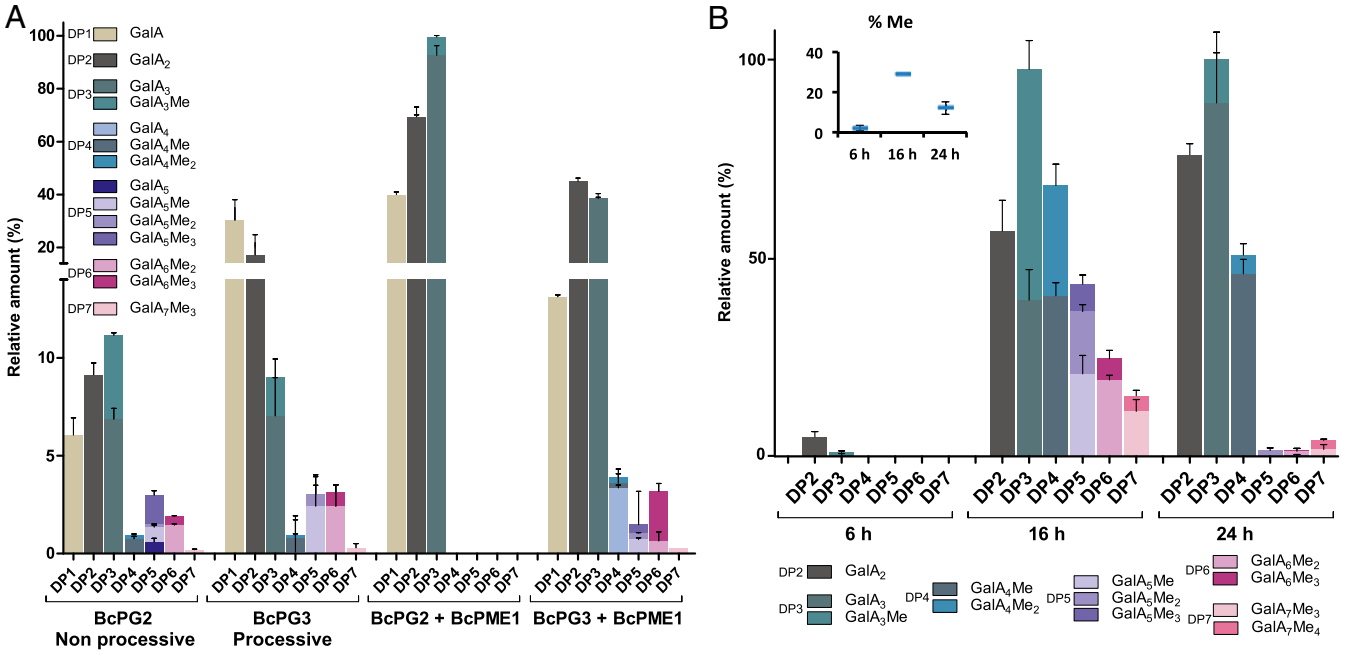

Fig. 2. OG analysis to characterize pectinolytic activities of *B. cinerea* on commercial citrus peel pectins. (*A*) Characterization of OGs by HP-SEC-MS released by BcPG2 and BcPG3 in the presence or absence of BcPME1 after 20 h of incubation with citrus pectins. Data are means ± SD; $n = 3$. (*B*) Kinetics of OGs produced by WT *B. cinerea* strain over time from citrus pectins and evolution of the OG methylesterification rate over time. Data are means ± SD; $n = 3$. OGs are named $GalA_xMe_y$. Subscript numbers indicate the degree of polymerization and the number of methylester groups.

Here we studied the OGs of *A. thaliana* leaves incubated with *B. cinerea* spores. The incubation was done in liquid medium since this facilitates the collection of large quantities of OGs. Under these conditions, the first plant symptoms can be observed between 9 and 12 h postinfection (hpi) (*SI Appendix*, Fig. S5). We chose 20 hpi to collect the medium, when significant maceration of the tissue was observed. After concentration, the medium was analyzed by HP-SEC. Whereas no OGs were detected in the control medium (*SI Appendix*, Fig. S6*A*), a complex OG mixture was observed upon infection with the spore suspension, which could be analyzed using in vitro-released OGs as standards. Surprisingly, the most abundant OGs detected in spore suspension at 20 hpi differed by 18 mass units (H_2O) from OGs released from citrus or sugar beet pectins (*SI Appendix*, Table S2). This difference was attributed to the loss of a water molecule between C4 and C5 of the nonreducing end GalA residue during the β-elimination reaction catalyzed by PNL (28). These OGs were named $GalA_xMe_yAc_z$-H_2O. We conclude that during infection, only 20% of the accumulated OGs were actually produced by PGs, the remaining 80% being the product of PNLs (Fig. 3*A*). This is in striking contrast with the OGs released by *B. cinerea* grown on citrus pectins, in which no PNL product was found (Fig. 2*B*).

Among the PNL products, 20 different OGs of DPs ranging from 3 to 10 were identified (Fig. 3*B*). The main products displayed a DP of 4 and 5, the $GalA_4MeAc$–H_2O being the most abundant, representing 25% of the OGs. To determine the precise position of the acetyl- and methylester groups on the $GalA_4MeAc$-H_2O, we analyzed the fragmentation pattern (*SI Appendix*, Fig. S7). The acetylester was only found on the A- and C-fragments, corresponding to the nonreducing end, but never on the Z-fragments, which correspond to the reducing end. Moreover, the ring cleavage product $^{0,2}A_1$ at 157.0051 *m/z* proves that the acetylesterification occurs on the C3 of the GalA at the nonreducing end. It is also worth noting that all of the PNL-generated OGs contained at least 1 GalAMe for 2 GalAs, some of them also being acetylesterified.

The PG-derived OGs were mainly of DP2 and -3. Surprisingly, DP3 OGs were all methylesterified and the bulk of the DP2 OGs was not $GalA_2$ but an ion at *m/z* 385, differing by 16 mass units (oxygen) from $GalA_2$ (369) (Fig. 3*C* and *SI Appendix*, Table S2). The MS/MS fragmentation pattern of this ion showed 2 major fragments corresponding to a uronic acid linked to a galactaric acid, which is a C1-oxidized uronic acid (Fig. 3*D*). To determine the origin of this oxidized $GalA_2$ ($GalA_2$ox), we performed a kinetic study of $GalA_3$, $GalA_2$, and $GalA_2$ox from 12 to 18 hpi. Whereas the amount of all 3 OGs increased from 12 to 15 hpi, $GalA_3$ and $GalA_2$ progressively disappeared in favor of $GalA_2$ox from 15 to 18 hpi (Fig. 3*E*). We assume that $GalA_3$ and $GalA_2$ are oxidized by a plant oxidase, as described recently (17). We also detected other oligosaccharides, the structure and origin of which were not investigated here.

The large proportion of PNL-derived OGs and the absence of long unmethylesterified OGs in infected leaves was surprising. To rule out that the OG profile was an artifact of the nonphysiological liquid culture system, we also analyzed the OGs released in spore suspension drops incubated for 24 h on detached *A. thaliana* leaves. Besides higher $GalA_2$ox levels, this shows OG structures that were similar to those detected in the culture medium of immersed leaves, albeit with differences in relative abundance of the OGs (*SI Appendix*, Fig. S6 *A* and *B*). These quantitative differences could reflect at least in part the less-advanced infection stage relative to that of immersed leaves. Then we incubated cell wall from *A. thaliana* leaves with *B. cinerea* spores and analyzed OGs produced over time. We showed that they all result from a PNL activity and not from a PG activity, suggesting that the accumulation of a large proportion of PNL-derived products during infection was due to *A. thaliana* pectin structure. It is worth noting that the main shortest OG was a DP6 and not a DP4, as observed during infection (*SI Appendix*, Fig. S8), suggesting that some plant enzyme activities might contribute to OG production upon infection.

To rule out that large OGs remained attached to the cell wall, we extracted residual OGs from the cell wall with a chelating agent. In these conditions only a major $GalA_2$ox peak was detectable (*SI Appendix*, Fig. S6*C*,) confirming that long and unmethylesterified OGs did not accumulate during infection. Finally, to determine why long and unmethylesterified OGs were not accumulated, we incubated OGs from DP3 to -15 with *B. cinerea* pregerminated spores and analyzed OGs over time. Surprisingly, as soon as the germinated fungus is in contact with these OGs, they were instantaneously hydrolyzed into shorter OGs (DP2 to -5) and to GalA, suggesting that $GalA_6$ to $GalA_{15}$ are too easily hydrolysable substrates for a *B. cinerea* arsenal to be accumulated during plant infection (Fig. 3*F*).

We next produced semipurified OG preparations from WT-infected leaves, enriched for $GalA_4MeAc$-H_2O (Fig. 3*G* and *SI Appendix*, Fig. S9) and which completely lacked the previously identified demethylesterified OG elicitors DP10 to -15 and DP3. $GalA_4MeAc$-H_2O represents 48% of total semipurified OGs from WT-infected leaves. The concentration of $GalA_4MeAc$-H_2O was determined by assuming that $GalA_3$ and $GalA_4MeAc$-H_2O response factors are equal. Incubation of *A. thaliana* leaves with OGs from infected leaves containing 5 μM of $GalA_4MeAc$-H_2O induced, within 3 h, a much higher expression of a defense reporter gene (*pAtPGIP1::GUS* [β-glucuronidase]) than in leaves and in hypocotyls incubated with $GalA_3$ (200 μM) preparation (Fig. 3 *H* and *I*). However, after a longer time of incubation (6 h), OG3 preparation induced a similar expression of *AtPGIP1* in etiolated hypocotyls except in vessels (Fig. 3*H*). This result supports the hypothesis that the plant may rapidly trigger its defense response upon recognition of PNL products,

A Fungal PNL Contributes to OG Production during Infection. We assumed that the PNL activity detected came from *B. cinerea*, since so far only PL and no PNL activity had been observed in plants (4). We therefore selected, from published transcriptome profiles (29), the most abundant transcript, encoding a putative PNL in germinating *B. cinerea* conidia (*BcPNL1*) to express the enzyme in *P. pastoris*. The enzyme, purified from the culture medium (*SI Appendix*, Fig. S10), showed PNL activity on various commercial substrates with a sharp optimum at pH 8 (Fig. 4*A*) and a preference for highly methylesterified pectins (Fig. 4*B*). To assess the potential role of this PNL in the production of unsaturated OGs during infection, we analyzed the OGs produced by this enzyme from *A. thaliana* leaf cell walls by HP-SEC-MS. We detected OGs from DP4, all methylesterified and some also acetylesterified (Fig. 4*C* and *SI Appendix*, Fig. S11). Among these OGs, 15 were also found in *B. cinerea*-infected *A. thaliana* leaves (Fig. 4*C* and *SI Appendix*, Fig. S11), while the other OGs were more methylesterified. Together, these results are consistent with the involvement of BcPNL1, in particular in the initial steps of OG production during *B. cinerea* infection.

Relative Contribution of the Main PG and PME Activities in Pectin Degradation during *B. cinerea* Growth. To gain better insights into OG production during *A. thaliana* leaf infection and to understand the role of these OGs in plant defense activation, we took advantage of *B. cinerea* mutants altered for each 1 of the 6 PGs and the double-mutant *Bcpme1/2* (22, 23). Unfortunately, we failed so far to produce a BcPNL1 mutant. qRT-PCR analysis showed that all of the *PG* and *PME* genes were expressed in WT *B. cinerea* grown in the presence of citrus pectins (*SI Appendix*, Fig. S12) after 6 and 16 h of incubation. We next analyzed the size of citrus pectins, using SEC, after 6-h incubation with the WT strain or each of the *Bcpg* and *Bcpme* mutants. Interestingly, multiple-angle light scattering, refractive index detection, and viscosimetry analyses (*SI Appendix*, Fig. S13) showed a larger size of digested pectins for all of the mutants relative to the WT strain, indicating that all of the investigated enzymes contributed to pectin digestion.

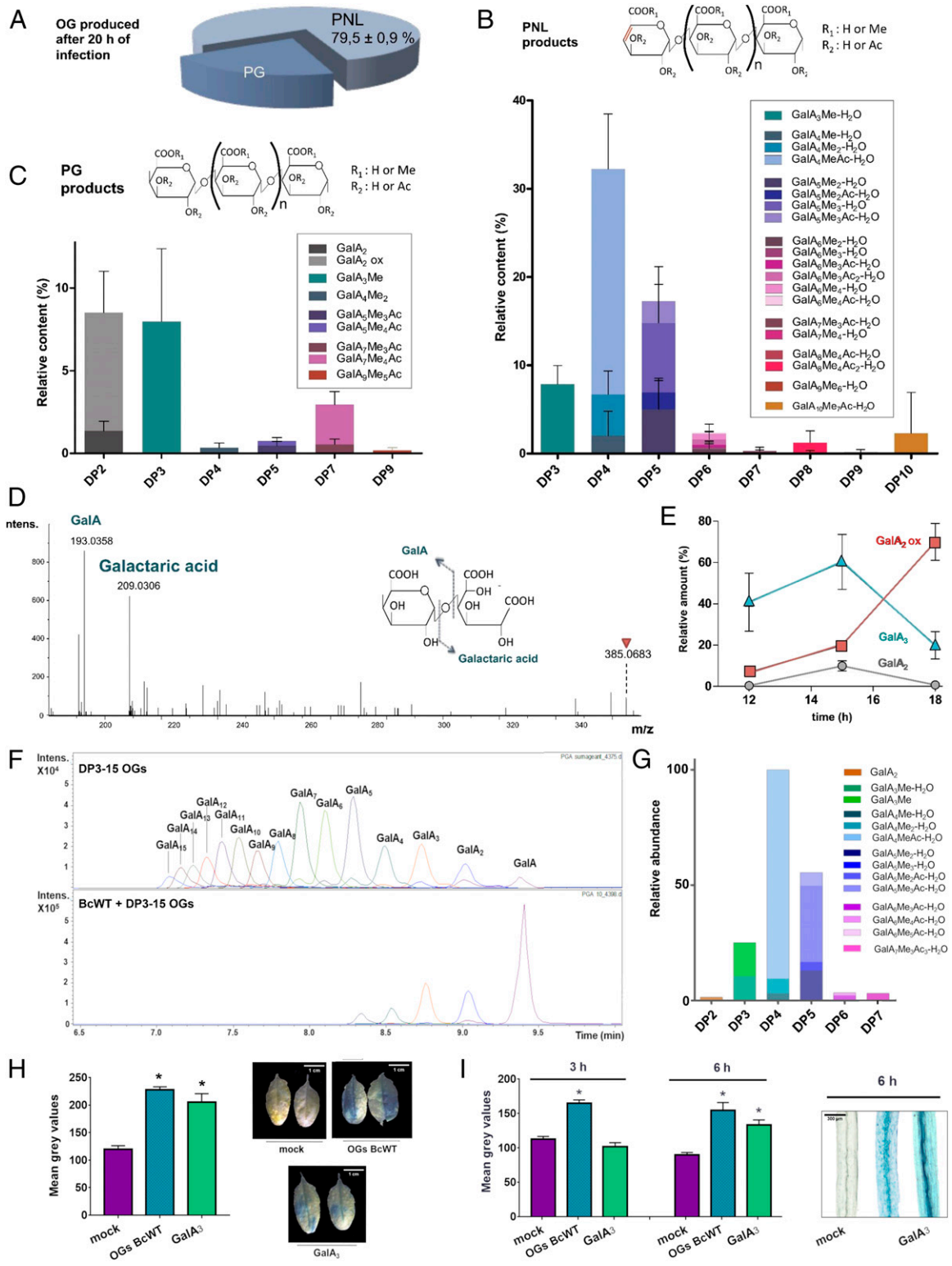

Fig. 3. OGs released upon *A. thaliana–B. cinerea* interaction. (*A*) Proportion of pectin lyase products among total OG produced after 20-h infection of *A. thaliana* leaves by *B. cinerea*. Data are means ± SD; $n = 3$. (*B* and *C*) Characterization of OGs produced after 20-h infection by HP-SEC-MS. (*B*) PNL products; (*C*) PG products. Data are means ± SD; $n = 3$. (*D*) MS^2 fragmentation pattern of oxydized $GalA_2$ oligomer (*m/z* 385.0683) eluting at 7.8 min in Fig. 1*A* using HP-SEC with online MS. (*E*) Kinetics of $GalA_3$, $GalA_2$, and oxydized $GalA_2$ upon infection. Data are means ± SD; $n = 3$. (*F*) DP10 to -15 OGs degradation by *B. cinerea*. OGs (2 mg/mL) were mixed with germinated *B. cinerea* spores and the reaction immediately stopped by addition of a volume of ethanol before analysis by HP-SEC-MS. (*G*) Composition of semipurified OGs from leaves infected by WT *B. cinerea* strain. (*H*) GUS quantification and staining of *A. thaliana* leaves expressing the promoter *PGIP1::GUS* fusion after the infiltration of $GalA_3$ (200 μM) and semipurified OGs containing 5 μM of $GalA_4MeAc\text{-}H_2O$. (*I*) GUS quantification and staining of *A. thaliana* dark-grown hypocotyls expressing the promoter *PGIP1::GUS* fusion after the infiltration of $GalA_3$ and semipurified OGs from leaves infected by WT *B. cinerea* strain. OGs are named $GalA_xMe_yAc_z$. Subscript numbers indicate the degree of polymerization and the number of methyl- and acetylester groups, respectively. Asterisks directly above bars denote statistical significance compared with mock treatment (*$P < 0.05$).

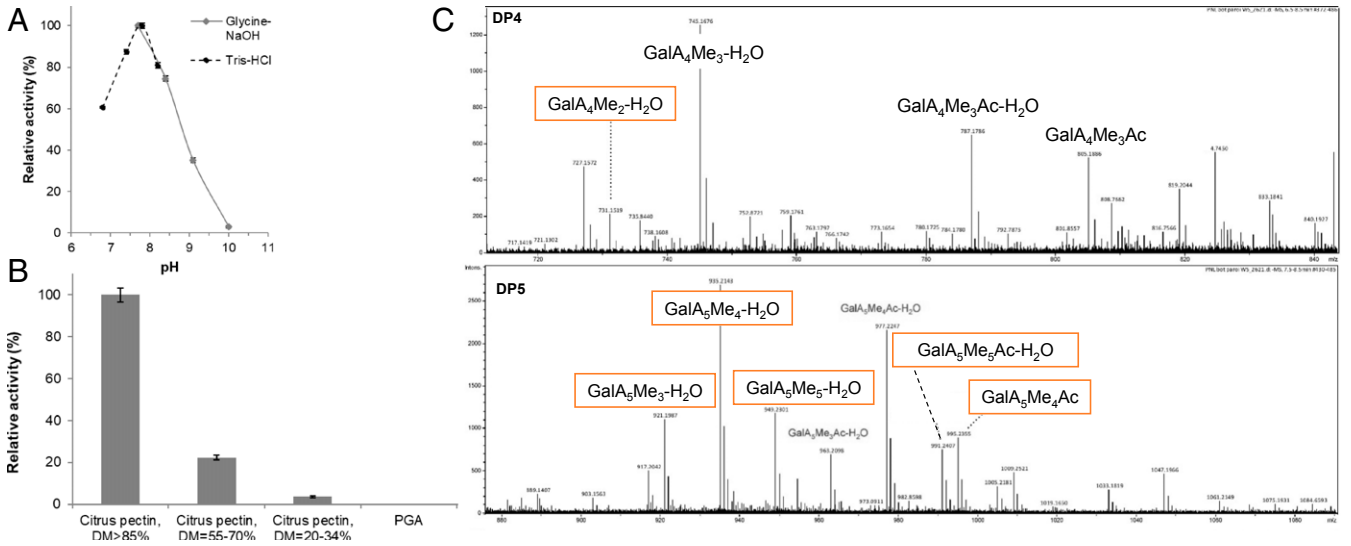

Fig. 4. BcPNL1 is active on highly methylesterified pectins and at alkaline pH. (*A*) PNL activity was measured at 235 nm at different pH, with glycine-NaOH and Tris·HCl buffers. Data represent the mean ± SE of 3 replicates. (*B*) PNL activity was measured at 235 nm using substrates with various DMs. Data represent the mean ± SE of 3 replicates. (*C*) OGs of DP4 and -5 released by BcPNL1 from *A. thaliana* leaf cell wall. Boxed OGs are found in infection OGs.

We also analyzed the OGs released after 16 and 24 h of *B. cinerea* mutant growth on citrus pectins. Principal component analysis (PCA) showed that after 16 h of growth *Bcpg1* and *Bcpme1/2* samples were separated from others (*SI Appendix*, Fig. S14*A*), and that at 24-hpi *Bcpme1/2* samples formed an independent group (*SI Appendix*, Fig. S14*B*). We scored the results for $\log_2$ fold-change compared to the WT strain (Fig. 5). After 16 h, *Bcpg1*, *Bcpme1/2*, and to a lesser extent *Bcpg2* were affected in OG production while no differences were observed for *Bcpg3* to *-6*. Interestingly, *Bcpme1/2* was the only mutant affected in $GalA_2$ production and showed higher levels of methylesterified OGs of DP6 and -7. After 24 h, *Bcpme1/2* accumulated, relative to the WT strain, even more methylesterified OGs of DP5 to -7 and less $GalA_3$ and $GalA_4Me$. In addition, all of the mutants, except *Bcpg1*, accumulated less $GalA_4Me$ than the WT strain, suggesting the involvement of all these enzymes in the production of this OG (Fig. 5). Interestingly, the large difference of the OGs released by *Bcpg1* relative to that released by the WT at 16 h had completely disappeared at 24 h. This indicates that BcPG1 was critical for the rate of OG accumulation, not for OG accumulation per se.

***Bcpg1* and *Bcpme1/2* Are Affected in OG Accumulation during Infection of *A. thaliana*.** We next investigated whether pectinolytic *B. cinerea* mutants were affected in OG accumulation also during infection of *A. thaliana* leaves. We focused on *Bcpg1* and *Bcpme1/2* since these mutants showed, in addition to compromised degradation of citrus pectins, the most perturbed OG profiles. *A. thaliana* leaves were infected with mutant and WT *B. cinerea* strains in liquid culture and the in vivo OGs were analyzed. HP-SEC-MS/MS analysis confirmed that OG production was affected in the 2 *B. cinerea* mutants also during infection of *A. thaliana* leaves (Fig. 6*A*). Indeed, for the WT strain, the relative OG composition evolved from 12 to 18 hpi. At 12 hpi, the OG size profile showed 2 peaks corresponding to large (>7) and small (3 to 5) DPs, respectively. The amounts of large DP OGs did not change during the time course. The amount of small OGs, however, strongly increased between 12 and 15 hpi and leveled off at 18 hpi. At this stage, a new peak corresponding to DP2 OGs ($GalA_2ox$) had appeared (Fig. 6*A*). In the mutants, the OG profile was strongly altered. First, whereas, like for the WT strain, the total amount of OGs increased over time, the relative OG composition did not evolve, suggesting that the enzymes encoded by the mutated genes were required for a specific step in the conversion of the OGs. For *Bcpme1/2*, more high-DP OGs accumulated relative to the WT strain, as observed on citrus pectins. In addition, DP4 levels were strongly reduced, DP5 to -10 accumulated and no DP2 accumulated at 18 hpi. BcPME activity therefore appears to be critical for the turnover of the large OGs, the production of DP4 OGs, and the conversion of OG into $GalA_2ox$. For *Bcpg1*, hardly any high DP OGs were

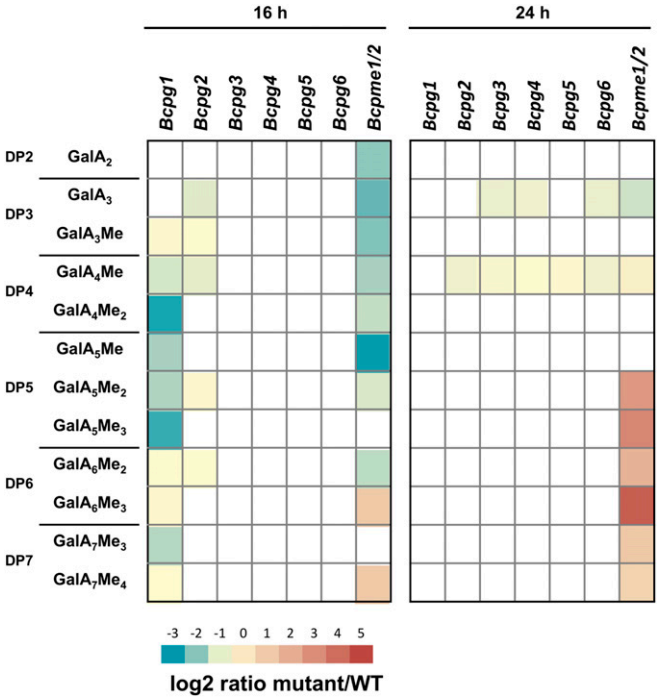

Fig. 5. *Bcpme1/2* and *Bcpg1* to *Bcpg6* strains are defective in citrus pectin digestion and *Bcpg1*, *Bcpg2*, and *Bcpme1/2* are impaired in OG production. OG production of *Bcpme1/2* and *Bcpg1* to *Bcpg6* mutants compared to WT strain after 16 and 24 h of citrus pectin digestion. OGs are named $GalA_xMe_y$. Subscript numbers indicate the DP and the number of methylester groups, respectively.

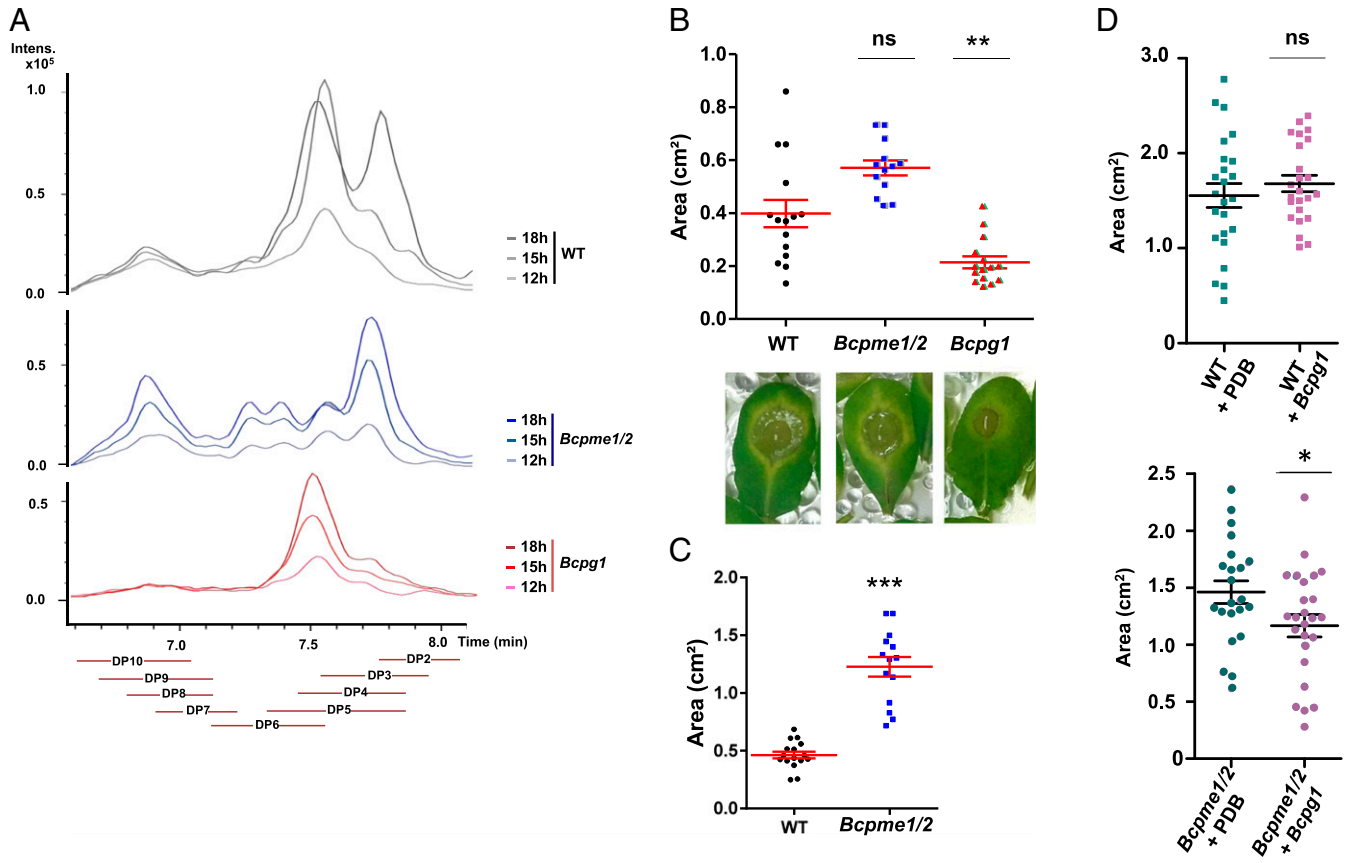

Fig. 6. Opposing effects of *Bcpg1* and *Bcpme1/2* mutations in virulence. (*A*) Extracted ion chromatograms obtained by HP-SEC-MS analysis in negative ionization mode of OGs endogenously produced during infection of *A. thaliana* leaves infected by WT *B. cinerea* strain and *Bcpg1*, *Bcpme1/2* mutants over time. (*B* and *C*) Infection assays of WT *B. cinerea* and mutant strains on 5-wk-old (*B*) or 6-wk-old (*C*) rosette leaves of *A. thaliana*. Statistical data of lesion size 72 hpi. Values are means ± SEM ($n = 15$); $^{**}P < 0.01$ and $^{***}P < 0.001$ by Student test. (*D*) *B. cinerea* coinfection assay on rosette leaves of *A. thaliana*. Leaves were infected with WT *B. cinerea* strain or *Bcpme1/2* followed 24 h later by *Bcpg1* or a mock control (PDB medium). Lesion size of the infected leaves were measured 72 h later. Values are means ± SEM ($n = 25$); $^{*}P < 0.05$ by Student test; ns: nonsignificant.

detected, again as observed on citrus pectins, and most OGs were of DP4, with very minor amounts of DP2 or DP3. BcPG1 activity therefore contributes to the generation of the large DP OGs but also to the turnover of DP4 OGs.

Opposing Effects of *Bcpg1* and *Bcpme1/2* Mutations on Virulence. *B. cinerea* infection assays showed low virulence for *Bcpg1* (24) and a comparable (after 72 hpi on young leaves) or a higher virulence (on older leaves) for *Bcpme1/2* (23), relative to the WT (Fig. 6 *B* and *C* and *SI Appendix*, Fig. S15).

Since both mutants are compromised in pectin turnover, the results indicate that the virulence of the fungus does not only reflect its capacity to degrade pectin (which, on first sight, might explain the reduced virulence of *Bcpg1*) but also its ability to prevent elicitation of the defense system of the plant. To test the latter possibility, we infected leaves with *Bcpme1/2* followed, 24 h later, by *Bcpg1* or a mock treatment (Fig. 6*D*). Interestingly, the presence of *Bcpg1* reduced the virulence of *Bcpme1/2*, relative to the mock control. No such effect was observed when *Bcpme1/2* was replaced by the WT strain in the experiment. These results led us to hypothesize that the increased virulence of *Bcpme1/2*, despite its impaired pectinolytic capacity, reflects opposing activities of the OGs in leaves infected with *Bcpme1/2* or *Bcpg1*/WT respectively.

OG Analysis Released by *B. cinerea* Mutants Identifies New Defense Elicitor and Suppressor Candidates. To identify differentially accumulating OGs that might explain such differences in virulence, we compared the OGs of *A. thaliana* leaves infected for 20 h (20 hpi) in liquid culture with *Bcpme1/2* or WT strains. PCA results revealed clustering of replicate samples and a clear separation between data from treatment by *Bcpme1/2* and WT strains, despite the higher variability among replicates in *Bcpme1/2*- relative to WT-infected conditions (*SI Appendix*, Fig. S16*A*). PCA on 72 OGs separated $GalA_2ox$ and $GalA_4MeAc\text{-}H_2O$ from the other OGs according to their relative abundance in the different samples (*SI Appendix*, Fig. S16*B*). Hierarchical cluster analysis on these OGs, after exclusion of $GalA_2ox$ from the comparison because of its high intragenotype variability (Fig. 7*A* and *SI Appendix*, Fig. S17), showed that $GalA_5Me_2Ac\text{-}H_2O/GalA_6Me_4\text{-}H_2O$ and $GalA_4MeAc\text{-}H_2O/GalA_3Me$ were, respectively, under- and overrepresented in leaves infected with the WT strain, as compared to *Bcpme1/2*. This suggests that demethylesterification by BcPME1/2 might be a critical step in the conversion of methylesterified DP5 and -6 OGs into shorter OG, presumably also involving an exo-PG activity. To investigate potential correlations between the enrichment in some OG and virulence, we first quantified the methylesterified DP4, -5, and -6 OGs in *Bcpg1*-, WT-, and *Bcpme1/2*-infected leaves (Fig. 7*B*). Interestingly, low methylesterified DP4 OG accumulated more in leaves infected with *Bcpg1* relative to the WT strain at 18 hpi, despite the reduced overall OG content in this mutant, and was barely detectable in *Bcpme1/2*. Opposingly, high methylesterified DP6 OG accumulated more in leaves infected with *Bcpme1/2* relative to the WT and *Bcpg1* strains.

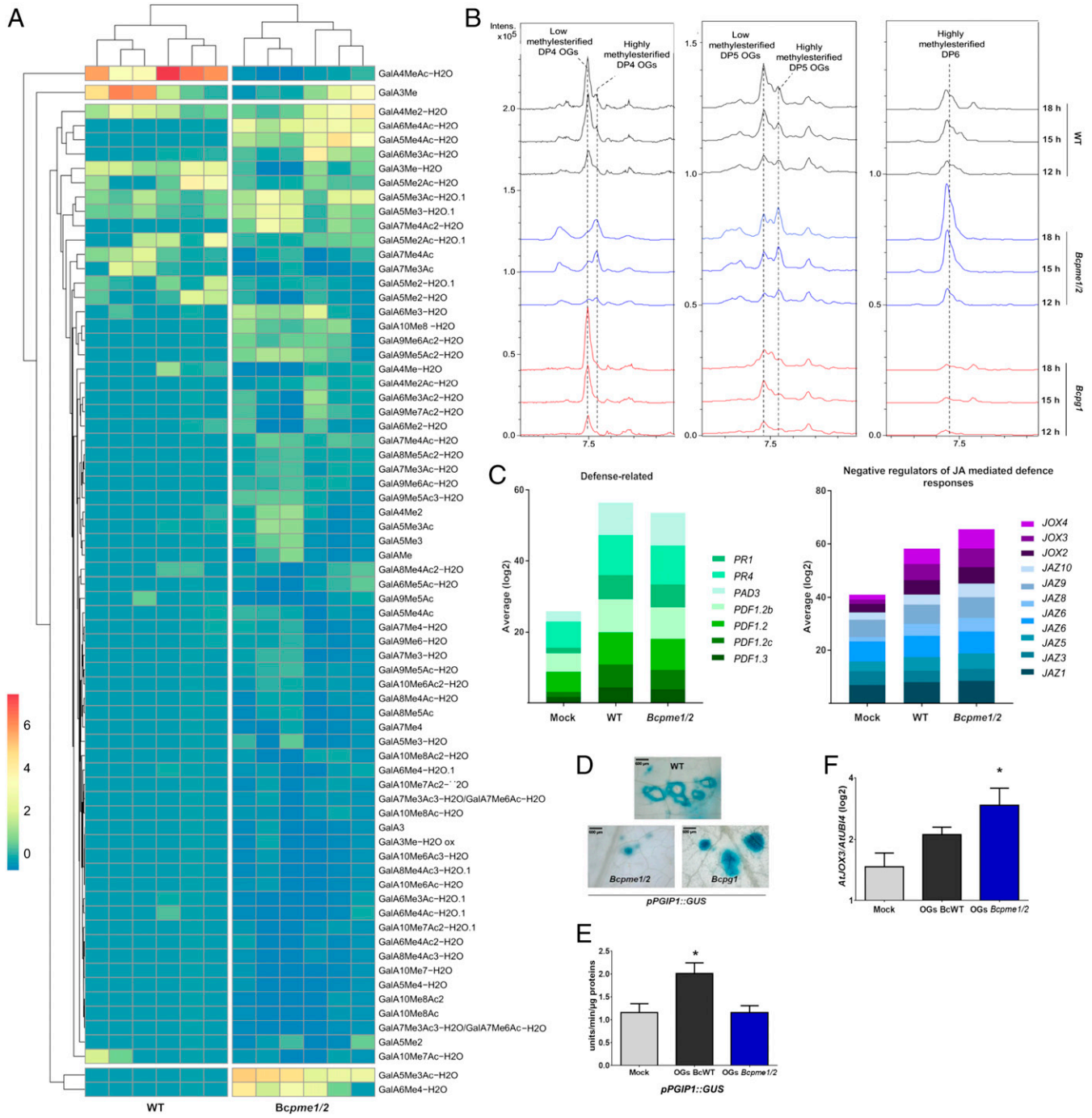

Fig. 7. The DP4/DP5 ratio of OGs produced by *Bcpg1*, *Bcpme1/2*, and WT *B. cinerea* strains correlates with their respective virulence. (*A*) Heatmap of all of the OGs (71 rows) for 12 samples (columns). Annotation labels refer to OG structure. Rows are centered; unit variance scaling is applied to rows. Both rows and columns are clustered using McQuitty distance and maximum linkage. (*B*) Extracted ion chromatograms for DP4, -5, and -6 OGs produced by *Bcpg1*, *Bcpme1/2*, and WT strains over time during infection of *A. thaliana* leaves. (*C*) Quantification of transcripts from JA and defense-related genes in noninfected leaves (mock) and leaves infected by WT and *Bcpme1/2* strains. Values of normalized transcript quantities from genes differentially expressed by WT or *Bcpme1/2* strains compared to noninfected leaves ($\log_2$, false-discovery rate F-test, P value < 0.01) are shown in Dataset S1. (*D*) GUS staining of *A. thaliana* leaves expressing the promoter *PGIP1::GUS* fusion after the infection of *Bcpme1/2*, *Bcpg1*, and WT strains. (*E*) GUS activity quantified by fluorescence in leaves from transgenic *A. thaliana* plants expressing the *GUS* reporter gene under the control of *AtPGIP1* promoter. Leaves were infiltrated by semipurified OGs from leaves either infected by *B. cinerea* WT strain or *Bcpme1/2*. Values are means ± SEM ($n = 6$); *$P < 0.05$ by Mann–Whitney *U* test (*F*) Expression of *AtJOX3* in leaves infiltrated by semipurified OGs from leaves either infected by *B. cinerea* WT strain or *Bcpme1/2*. Values are means ± SEM ($n = 4$); *$P < 0.05$ by Mann–Whitney *U* test. OGs are named $GalA_xMe_yAc_z$. Subscript numbers indicate the DP and the number of methyl- and acetylester groups, respectively.

The negative correlation between short OG levels and fungal virulence might indicate an elicitor specific activity for these OGs as opposed to longer-than-DP4 OGs that might have a defense-suppressor activity. The timing of appearance of these different OGs may also be of importance for the virulence of the different strains. To clarify the role of these different OGs, we compared the transcriptomes of leaves infected for 24 h with WT or *Bcpme1/2*, when symptoms were already visible. Comparison of fungus- (WT or

Bcpme1/2) with mock-infected leaves revealed a total of 7,395 differentially expressed *A. thaliana* genes (Dataset S1), many of which were annotated as "defense related," involved in "protein processing in endoplasmic reticulum" or in "phenylpropanoid biosynthesis" (Fig. 7*C* and *SI Appendix*, Fig. S18). Among those, the pool of transcripts encoding negative regulators of JA signaling [JOX proteins hydroxylate and inactivate JA (30, 31) and JAZ proteins are transcriptional repressors of JA-regulated genes] (32) was slightly upregulated in leaves infected with *Bcpme1/2* relative to the WT strain (Fig. 7*C*), suggesting that the *Bcpme1/2* strain might suppress the plant defense mechanism. This did not simply reflect a more advanced infection stage of *Bcpme1/2*, since transcript levels for other defense-related genes were comparable, if not slightly lower, in *Bcpme1/2* vs. WT-infected leaves. As mirrored in the enhanced and reduced induction of a defense reporter gene (*pPGIP1::GUS*) in response to infection with *Bcpg1* and *Bcpme1/2*, respectively, relative to the WT strain (Fig. 7*D*), this suggests that, among the immune responses elicited by the fungus, JA-dependent defenses are induced more efficiently by the WT strain than by *Bcpme1/2*.

Finally, to test if low methylesterified DP4 OGs contribute to the plant defense elicitation and if highly methylesterified longer-than DP4 OGs contribute to the circumvention of plant defense mechanisms, we partially purified a mix of methylesterified OGs produced by BcWT and *Bcpme1/2* (see *SI Appendix*, Fig. S19 for OG composition). First, we infiltrated leaves of transgenic *A. thaliana* plants transformed with the *GUS* reporter gene under the control of the *AtPGIP1* promoter that is induced by trimers and long OG (DP10 to -15). Our results showed that at 24 h post-infiltration, *AtPGIP1* is twice more activated by $GalA_4MeAc\text{-}H_2O$–enriched extract than with OGs produced by *Bcpme1/2* (Fig. 7*E*). Second, we infiltrated *A. thaliana* leaves with these different OG mixes and monitored the expression of the *JOX3* gene, which is involved in JA degradation. *JOX3* was activated 3 h after the infiltration of OG purified from *Bcpme1/2*-infected leaves, enriched in highly methylesterified DP5 and -6 OGs, suggesting that these OGs may contribute to circumvent plant defense (Fig. 7*F*).

In conclusion, OG analysis revealed the presence of complex mixtures of OGs that are different from the previously described ones, and the nature and accumulation may be critical for the effectiveness of the immune response against *B. cinerea*, at least in part by affecting defense gene expression patterns *in planta*.

Discussion

This study showed that HP-SEC provides a high-resolution separation method, which is based on the DP, degree of acetylation, DM, and even the methylesterification pattern of the OGs and superior to commonly used HILIC-based methods (19–21). The OGs obtained with this method allowed the study of the mode of action of specific pectin-modifying enzymes, in vivo pectinolytic activity, OGs produced during plant–microbe interactions, and the identification of new cell wall-derived DAMP candidates.

The complexity of the OGs released upon in vivo plant–fungus interactions appears to reflect, to a large extent, the battleground of fungal pectinolytic activities and plant-defense strategies. For example, it was striking to see that unmethylesterified OGs of DP10 to -15 were absent in *B. cinerea*-infected citrus pectins or *A. thaliana* leaves while they have been detected in noninoculated leaves and in *A. thaliana* upon coexpression of a PGIP with a fungal PG (27, 33). They have, until now, been considered important DAMPs for necrotrophic pathogens and are frequently used in the study of defense responses (6–12). In *B. cinerea* grown on citrus pectins, the fungal enzymatic machinery rapidly converted PG products into GalA, $GalA_2$, and $GalA_3$, whereas higher DP OGs accumulated only in a methylesterified form. Similarly, germinated spore enzymes instantly convert long OGs (DP5 to -15) into shorter OGs. In *B. cinerea*-infected leaves, most PG products were converted into $GalA_3Me$ and $GalA_2ox$. The production of the latter OGs presumably involved plant-produced OG oxidases (OGOX) (17, 34, 35) of the berberine bridge enzyme family. Oxidized OGs are more recalcitrant to the hydrolysis of fungal enzymes and, interestingly, plants overexpressing OGOX1 are more resistant to *B. cinerea*. In our experimental settings, $GalA_2ox$ accumulated at late infection stages (between 15 and 18 hpi) concomitantly with the reduction of $GalA_3$ and $GalA_2$ levels, which suggests that OG oxidase activity is induced only once the invader is detected. The exact role for $GalA_2ox$, however, remains to be demonstrated. Oxidation was shown to decrease the elicitor effect of OGs (17), in which case the enzyme activity may actually contribute to preventing OG-induced cell death during the necrotroph infection. Alternatively, the molecule itself or the H_2O_2 that is produced during the oxidation reaction may have signaling activity. Another strategy of the fungus to limit defense responses may be the suppression of unmethylesterified $GalA_3$ (another defense-response elicitor) (14) in *B. cinerea*-infected leaves relative to infected citrus pectins. This implies the existence, in *B. cinerea*-infected leaves, of an efficient PG activity able to hydrolyze such trimers, which might be BcPG3 (23).

This study showed that the overall OG profiles generated by *B. cinerea* grown on citrus pectins and on *A. thaliana* leaf cell wall were strikingly different. The former was exclusively the result of the hydrolytic activity of PGs, whereas the latter were for 80% the product of fungal PNL activity. The greatly reduced PG activity in the presence of *A. thaliana* cell wall would be the result of highly methylesterified and acetylated pectins.

One interesting application of the OG analysis in this study was the screening for novel OG DAMPs. The comparison of OGs of leaves infected with the WT strain or the mutants *Bcpg1* and *Bcpme1/2*, which both showed reduced pectinolytic activity but decreased and increased virulence, respectively, showed a negative correlation between virulence and the presence and timing of appearance of short (DP3 to -4) low methylesterified OGs during infection. Semipurified OG fraction from infected leaves by the WT strain was able to induce defense-gene expression, indicating the presence in the mixture of OGs with DAMP activity, which are different from the previously reported unmethylesterified $GalA_{10–15}$ or $GalA_3$. Similarly, long and highly methyl- and acetylesterified OGs were able to induce the *JOX3* gene, which is involved in JA degradation and suggests that these OGs are potential defense suppressors.

The final demonstration that some OGs have specific activities, like the induction or the suppression of defense responses, will await the in vitro production and purification of these OGs. This will be greatly facilitated by the identification in this work of the fungal enzymes that contribute to the generation of this OG. Indeed BcPNL1 (and perhaps 1 or more of the other 4 *B. cinerea* PNLs) generates, from *A. thaliana* cell walls, methylesterified OGs > DP4 with an unsaturated, often acetylesterified, GalA residue at the nonreducing end. The absence of $GalA_4MeAc\text{-}H_2O$ in *Bcpme1/2* indicates the involvement of 1 or both PMEs in the demethylesterification of a precursor molecule. This may be $GalA_5Me_3Ac\text{-}H_2O$, which selectively accumulated during infection by this mutant. It is conceivable that the PMEs remove 2 methyl groups from this molecule while leaving 1 methyl at position 3. A PG activity could then remove 1 GalA residue from the reducing end to yield $GalA_4MeAc\text{-}H_2O$. Finally, the accumulation of $GalA_4MeAc\text{-}H_2O$ in *Bcpg1* indicates that BcPG1 is required for the turnover of the molecule, in particular during early infection stages.

In conclusion, this study provides an extension of the omics toolbox with a method for the global analysis of the OGs that are produced during plant–pathogen interactions. This method will allow the study of other cell wall-derived signaling molecules involved in development and in abiotic stress responses, to investigate the evolution of enzymatic interactions between plants and their microbial environment, and may lead to the development of new strategies for the protection of crops against pathogens (36).

Materials and Methods

For full and detailed methods, please see *SI Appendix, Materials and Methods*.

Plant Material and Fungal Strains. *A. thaliana* WT Wassilewskija (Ws-0) plants were grown in soil in a growth chamber at 22 °C, 70% humidity, under irradiance of 100 $\mu mol \cdot m^{-2} \cdot s^{-1}$ with a photoperiod of 8-h light/16-h dark. Leaves or pectins were incubated with different strains of *B. cinerea* named B05.10 *Bcpg1-6* and *Bcpme1/2*.

OG Characterization and Quantification. Samples were analyzed by using chromatographic separation on an ACQUITY UPLC Protein BEH SEC Column and MS-detection performed in negative mode.

ACKNOWLEDGMENTS. This work was supported by grants from the Agence Nationale de la Recherche (ANR-12-BSV5-0001 GALAPAGOS and ANR-14-CE34-0010-03 PECTOSIGN projects) and the Laboratoire d'Excellence "Saclay Plant Science" project "Dynano." The financial support from the Institut Universitaire de France (to J.P.) is gratefully acknowledged. The authors benefited from the Institut Jean-Pierre Bougin Plant Observatory facilities. The Institut Jean-Pierre Bougin benefits from the support of the LabEx Saclay Plant Sciences-SPS (ANR-10-LABX-0040-SPS). We thank J. Van Kan for providing *Bcpg1-6* and *Bcpme1/2* mutant strains; G. De Lorenzo for providing the *A. thaliana pAtPGIP1::GUS* line; P. Lerouge for critical reading of the manuscript; and T. Elmayan is thanked for helping with the GUS quantification.

1. P. Albersheim *et al.*, "Oligosaccharins: Naturally occurring carbohydrates with biological regulatory functions" in *Structure and Function of Plant Genomes*, O. Ciferri, L. Dure, Eds. (Springer, New York, 1983), pp. 293–312.
2. J. A. L. van Kan, Licensed to kill: The lifestyle of a necrotrophic plant pathogen. *Trends Plant Sci.* **11**, 247–253 (2006).
3. B. L. Ridley, M. A. O'Neill, D. Mohnen, Pectins: Structure, biosynthesis, and oligogalacturonide-related signaling. *Phytochemistry* **57**, 929–967 (2001).
4. F. Sénéchal, C. Wattier, C. Rustérucci, J. Pelloux, Homogalacturonan-modifying enzymes: Structure, expression, and roles in plants. *J. Exp. Bot.* **65**, 5125–5160 (2014).
5. L. Hocq, J. Pelloux, V. Lefebvre, Connecting homogalacturonan-type pectin remodeling to acid growth. *Trends Plant Sci.* **22**, 20–29 (2017).
6. M. G. Hahn, A. G. Darvill, P. Albersheim, Host-pathogen interactions: XIX. The endogenous elicitor, a fragment of a plant cell wall polysaccharide that elicits phytoalexin accumulation in soybeans. *Plant Physiol.* **68**, 1161–1169 (1981).
7. E. Melotto, L. C. Greve, J. M. Labavitch, Cell wall metabolism in ripening fruit (vii. Biologically active pectin oligomers in ripening tomato (*Lycopersicon esculentum* Mill.) fruits). *Plant Physiol.* **106**, 575–581 (1994).
8. J. Messiaen, N. D. V. Read, P. Van Cutsem, A. J. Trewavas, Cell wall oligogalacturonides increase cytosolic free calcium in carrot protoplasts. *J. Cell Sci.* **104**, 365–371 (1993).
9. R. Moscatiello, P. Mariani, D. Sanders, F. J. M. Maathuis, Transcriptional analysis of calcium-dependent and calcium-independent signalling pathways induced by oligogalacturonides. *J. Exp. Bot.* **57**, 2847–2865 (2006).
10. S. Ferrari *et al.*, Resistance to *Botrytis cinerea* induced in Arabidopsis by elicitors is independent of salicylic acid, ethylene, or jasmonate signaling but requires PHYTOALEXIN DEFICIENT3. *Plant Physiol.* **144**, 367–379 (2007).
11. C. Denoux *et al.*, Activation of defense response pathways by OGs and Flg22 elicitors in Arabidopsis seedlings. *Mol. Plant* **1**, 423–445 (2008).
12. T. Moloshok, G. Pearce, C. A. Ryan, Oligouronide signaling of proteinase inhibitor genes in plants: Structure-activity relationships of Di- and trigalacturonic acids and their derivatives. *Arch. Biochem. Biophys.* **294**, 731–734 (1992).
13. S. D. Simpson, D. A. Ashford, D. J. Harvey, D. J. Bowles, Short chain oligogalacturonides induce ethylene production and expression of the gene encoding aminocyclopropane 1-carboxylic acid oxidase in tomato plants. *Glycobiology* **8**, 579–583 (1998).
14. P. Davidsson *et al.*, Short oligogalacturonides induce pathogen resistance-associated gene expression in Arabidopsis thaliana. *BMC Plant Biol.* **17**, 19 (2017).
15. S. A. Sinclair *et al.*, Etiolated seedling development requires repression of photomorphogenesis by a small cell-wall-derived dark signal. *Curr. Biol.* **27**, 3403–3418.e7 (2017).
16. H. J. An *et al.*, Determination of pathogen-related enzyme action by mass spectrometry analysis of pectin breakdown products of plant cell walls. *Anal. Biochem.* **338**, 71–82 (2005).
17. M. Benedetti *et al.*, Four Arabidopsis berberine bridge enzyme-like proteins are specific oxidases that inactivate the elicitor-active oligogalacturonides. *Plant J.* **94**, 260–273 (2018).
18. G. A. Luzio, R. G. Cameron, Determination of degree of methylation of food pectins by chromatography. *J. Sci. Food Agric.* **93**, 2463–2469 (2013).
19. C. Remoroza *et al.*, Combined HILIC-ELSD/ESI-MS(n) enables the separation, identification and quantification of sugar beet pectin derived oligomers. *Carbohydr. Polym.* **90**, 41–48 (2012).
20. A. G. M. Leijdekkers, M. G. Sanders, H. A. Schols, H. Gruppen, Characterizing plant cell wall derived oligosaccharides using hydrophilic interaction chromatography with mass spectrometry detection. *J. Chromatogr. A* **1218**, 9227–9235 (2011).
21. C. Remoroza, H. C. Buchholt, H. Gruppen, H. A. Schols, Descriptive parameters for revealing substitution patterns of sugar beet pectins using pectolytic enzymes. *Carbohydr. Polym.* **101**, 1205–1215 (2014).
22. A. ten Have, W. O. Breuil, J. P. Wubben, J. Visser, J. A. L. van Kan, *Botrytis cinerea* endopolygalacturonase genes are differentially expressed in various plant tissues. *Fungal Genet. Biol.* **33**, 97–105 (2001).
23. I. Kars, M. McCalman, L. Wagemakers, J. A. L. VAN Kan, Functional analysis of *Botrytis cinerea* pectin methylesterase genes by PCR-based targeted mutagenesis: Bcpme1 and Bcpme2 are dispensable for virulence of strain B05.10. *Mol. Plant Pathol.* **6**, 641–652 (2005).
24. A. ten Have, W. Mulder, J. Visser, J. A. L. van Kan, The endopolygalacturonase gene *Bcpg1* is required for full virulence of *Botrytis cinerea*. *Mol. Plant Microbe Interact.* **11**, 1009–1016 (1998).
25. I. Kars *et al.*, Necrotizing activity of five Botrytis cinerea endopolygalacturonases produced in Pichia pastoris. *Plant J.* **43**, 213–225 (2005).
26. G. De Lorenzo, S. Ferrari, Polygalacturonase-inhibiting proteins in defense against phytopathogenic fungi. *Curr. Opin. Plant Biol.* **5**, 295–299 (2002).
27. M. Benedetti *et al.*, Plant immunity triggered by engineered in vivo release of oligogalacturonides, damage-associated molecular patterns. *Proc. Natl. Acad. Sci. U.S.A.* **112**, 5533–5538 (2015).
28. R. J. Linhardt, P. M. Galliher, C. L. Cooney, Polysaccharide lyases. *Appl. Biochem. Biotechnol.* **12**, 135–176 (1986).
29. M. Leroch *et al.*, Transcriptome profiling of Botrytis cinerea conidial germination reveals upregulation of infection-related genes during the prepenetration stage. *Eukaryot. Cell* **12**, 614–626 (2013).
30. L. Caarls *et al.*, *Arabidopsis* JASMONATE-INDUCED OXYGENASES down-regulate plant immunity by hydroxylation and inactivation of the hormone jasmonic acid. *Proc. Natl. Acad. Sci. U.S.A.* **114**, 6388–6393 (2017).
31. E. Smirnova *et al.*, Jasmonic acid oxidase 2 hydroxylates jasmonic acid and represses basal defense and resistance responses against *Botrytis cinereal* infection. *Mol. Plant* **10**, 1159–1173 (2017).
32. F. Zhang *et al.*, Structural basis of JAZ repression of MYC transcription factors in jasmonate signalling. *Nature* **525**, 269–273 (2015).
33. D. Pontiggia *et al.*, Sensitive detection and measurement of oligogalacturonides in Arabidopsis. *Front. Plant Sci.* **6**, 258 (2015).
34. R. Pressey, Oxidized oligogalacturonides activate the oxidation of indoleacetic Acid by peroxidase. *Plant Physiol.* **96**, 1167–1170 (1991).
35. D. Cantu, L. C. Greve, S. Lurie, J. M. Labavitch, Detection of uronic oxidase activity in ripening peaches. *Phytochemistry* **67**, 13–18 (2006).
36. D. Expert *et al.*, *Dickeya dadantii* pectic enzymes necessary for virulence are also responsible for activation of the *Arabidopsis thaliana* innate immune system. *Mol. Plant Pathol.* **19**, 313–327 (2018).